



## The Tilted Solar Magnetic Dipole

A.A. Norton, G.J.D. Petrie & N.-E. Raouafi

**A**strophysical bodies often have magnetic axes not aligned with their rotational axes. For instance, the magnetic axes of Earth and Uranus have tilt angles of  $11^\circ$  and  $60^\circ$  with respect to their rotational axes. The Earth's magnetic field is attributed to interactions between the solid iron core, the outer molten core, and planetary rotation (Coe and Glatzmaier, 2006). Modeling shows that the same process (convection in a rotating shell of conducting fluid) can explain all dynamo-generated magnetic fields (Stanley and Bloxham, 2004). Another explanation is a primordial magnetic field, i.e., an axis direction 'frozen in' during formation.

The Sun has a magnetic dynamo acting in the interior, with toroidal bands of magnetism at the base of the convection zone being the source of sunspots. In discussing a "magnetic axis," we refer directly to the dipole component of the magnetic field. Of course, there are higher-order moments that are strongest near solar maximum, but their effect is more important at lower latitudes. As sunspots evolve and decay, flux is transported to the high latitudes, causing the polar magnetic reversal (Durrant, et al., 2004).

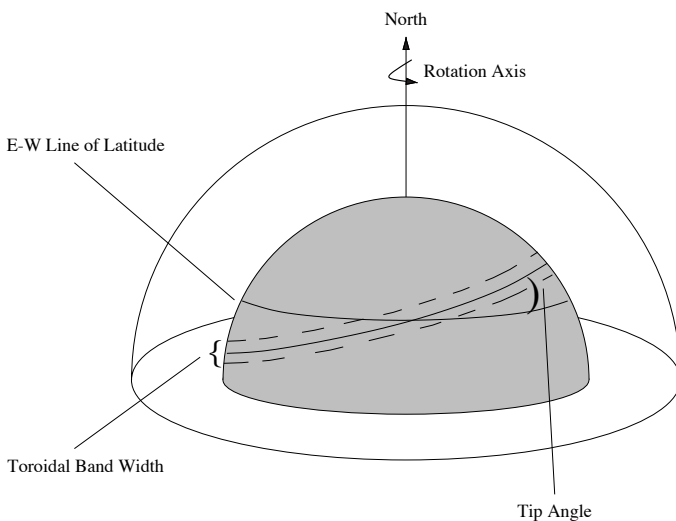


**Figure 1:** Schematic depicting only the Northern solar hemisphere, with the equator at the bottom. The toroidal band is tipped with respect to lines of constant latitude. The outer half-sphere represents the photosphere. The inner half-sphere represents the base of the convection zone.

We examine the tilt of the solar magnetic dipole near the 1996 solar minimum. We are motivated by the idea that a persistent tilted dipole may result from an MHD instability acting upon the toroidal magnetic bands in the interior (see figure 1). Non-axisymmetric eruption of sunspots mapping out an  $m=1$  (or 'tilted band') pattern in longitude has been predicted by dynamo theory and observed in sunspot location patterns (Norton and Gilman, 2004). The decay of the

follower spots and the pole-ward migration of flux could create polar caps misaligned with the N-S rotational axis (see figure 2).

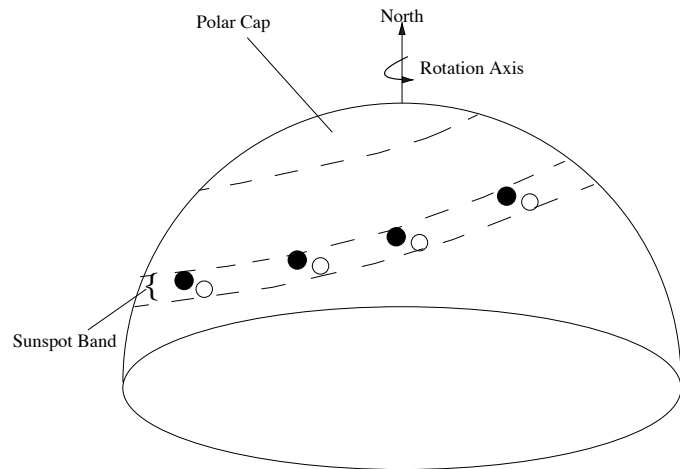


**Figure 2:** Sunspot locations trace out the location of the tipped toroidal band. Note, the angle is exaggerated compared to the expected  $5-10^\circ$ . An off-axis polar cap could result. We propose that this mechanism could cause the solar magnetic poles to be offset from the rotational axis.

Coronagraph data from the Large Angle and Spectrometric Coronagraph Experiment (LASCO) are used to study the global coronal geometry for Carrington Rotations (CRs) 1900-1932 (Brueckner, et al., 1995). During this time, the streamers observed in the corona trace out the neutral line and the heliospheric current sheet is in its most simple configuration (Wilcox & Hundhausen, 1983). The streamer belts are seen in white light images as bright cusps initiating in the mid-latitudes, with cusp closure near the equator.

Simultaneously observed East and West limb streamer profiles are compared by cross-correlating the brightness as a function of latitude. To display the evolution of the dipole tilt, we plot the latitudinal displacement as a function of time (see figure 3). A damped sinusoidal pattern results for CRs 1915-1919, indicative of a dipole tilt with amplitude decreasing in time, which may be a signature of the descent toward solar minimum.

We also investigate the center-of-gravity (COG) of the magnetic polar caps and the polar coronal holes. We use Kitt Peak Vacuum Tower (KPVT) magnetograms and SoHO Extreme Ultraviolet Imaging Telescope data. To determine the COG, the edges of the polar holes are selected visually, with coordinates translated into latitude and longitude. A similar method is employed for the magnetic polar caps. For comparison, we use the potential-field source-surface (PFSS)

*continued*

*The Tilted Solar Magnetic Dipole continued*

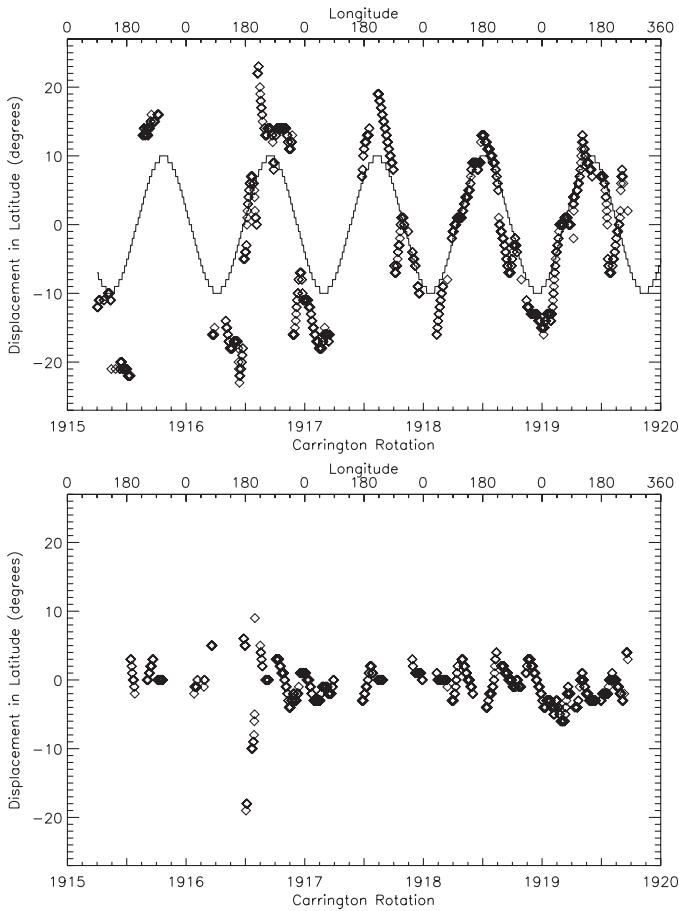


**Figure 3:** The displacement in latitude that results in the best cross correlation between streamers on the East and West limb of the sun (diamonds). A periodic signal is expected from a dipole geometry tilted with respect to the rotational axis. A 10° tilt is overplotted as a solid line for reference.

model, with KPVT magnetogram data as input, to model the coronal hole boundaries and the magnetic dipole term (see figure 4).

This research represents an effort to connect the current understanding of the dynamic magnetic field at the base of the convection zone with non-axisymmetry observed in solar surface magnetism. The mechanism outlined in figures 1–2 could contribute up to 10° to the tilt of the magnetic dipole. The equatorial streamers map out a sinusoidal structure in longitude and latitude about the equator for CR 1915–1919 with ~10° amplitude in latitude. The polar caps defined by the coronal holes and modeling exhibit a tilt with values ranging from 1 to 10° with an average value of 4–6°.

These are acceptable amplitudes to result from the MHD instability of the toroidal bands. However, without the polar cap geometries determined from the unipolar magnetic regions as seen in surface flux (and not just as determined from the polar hole locations), the viability of

the proposed mechanism for creating a non-zero magnetic dipole tilt at solar minimum remains in question. For a more in-depth treatment on this topic, see Norton and Raouafi, 2008 and Norton, Petrie and Raouafi, 2008.

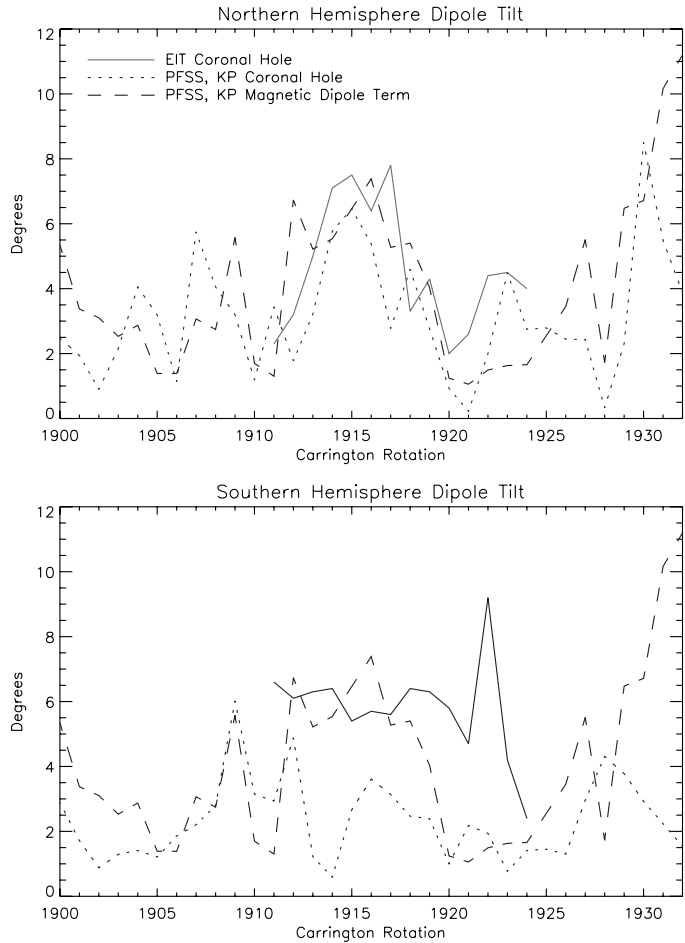


**Figure 4:** The tilt of the polar caps COG is plotted for CRs 1910–1932 determined from the observed coronal holes (red), the coronal holes from PFSS models (green), and the dipole terms (blue). [See online version for full color.] The values as calculated from the KPVT synoptic maps were determined to be too noisy.

Coe, R. and Glatzmaier, G., 2006, *Geophysical Research Letters*, **33**, 21  
 Durrant, C.J., Turner, J.P.R., and Wilson, P.R., 2004, *Solar Physics*, **222**, 345  
 Norton, A.A. and Gilman, P.A., 2005, *Astrophysical Journal*, **630**, 1194  
 Norton, A.A., and Raouafi, N.-E., 2008, *ASP Conf. Series*, **383**, 405  
 Norton, A.A., Petrie, G.J.D., and Raouafi, N.-E., 2008, *Astrophysical Journal*, in press  
 Stanley, S. and Bloxham, J., 2004, *Nature*, **428**, 151–153  
 Wilcox, J.M. and Hundhausen, A.J., 1983, *Journal of Geophysical Research*, **88**, 8095



## Watching the Production of Elements in Evolved Stars continued


with the Phoenix spectrograph at Gemini South analyzed with our hydrostatic model atmospheres revealed for the first time an observed increase of both ratios as stars evolve up the AGB. The findings nicely agree with our model expectations as shown in figure 2.

However, as it is often the case in science, our results allude to topics not expected at the planning phase of a project. Of particular interest is our finding that the  $^{12}\text{C}/^{13}\text{C}$  ratio reaches a saturation level close to 60 for high C/O ratios (especially for  $\text{C}/\text{O} > 1$ ). This cannot be explained by the standard model, which would suggest a steady increase of  $^{12}\text{C}/^{13}\text{C}$ . Thus a way for producing  $^{13}\text{C}$  during these late stages is required. The most obvious explanation for this observational pattern is the occurrence of a mixing process able to bridge the radiative gap between the cool bottom of the convective envelope and the hot H-burning zone. A similar process has been posited to explain some abundance anomalies in red giant stars (e.g., see Charbonnel 1995, Nollett et al., 2003).

In spite of much observational evidence, a common consensus on the physical mechanism driving this mixing has not been established (explanations include rotational induced instabilities, magnetically induced circulation, gravity waves or thermohaline mixing). The

scenario emerging from the evolutionary sequence of  $^{12}\text{C}/^{13}\text{C}$  versus C/O in NGC 1846 is that of a moderate deep mixing, affecting the  $^{13}\text{C}$  surface abundance in the late part of the AGB only, when stars become C-rich. The abundance derived from O-rich stars in NGC 1846 are all compatible with the predictions of models with no extra mixing. In figure 2, models including this effect are also shown. Our observations set new constraints on the amount of matter and the maximum temperature reached by this mixing, and will help to reveal the nature of this effect.

Finally, the near-infrared spectra obtained at Gemini South allowed measuring the abundance changes of the light element fluorine, whose nucleosynthetic origin is not understood. We demonstrate that the fluorine abundance increases with C/O, strongly favoring AGB stars as the source of fluorine in the Universe.

Using the Phoenix spectrograph at Gemini South again during the previous two semesters, we are extending our study to a few other LMC clusters in order to test the effects of different mass and metallicity on the mixing. Data analysis is under way and we expect to be able to present further results in the near future. 

# The Magellanic Bridge: Tidal Debris in our Backyard

Jason Harris

The silent expanse of our intergalactic neighborhood is occupied by a few dozen small galaxies. The largest and most enigmatic of these dwarf satellites are the Large and Small Magellanic Clouds (LMC and SMC), a pair of galaxies whose star-formation histories have likely been driven by their mutual gravitational dance. On a timescale that is both incomprehensibly vast and cosmologically tiny, the LMC and SMC embrace, spin, and dip as they plunge through a complex and ever-changing repertoire of interplay.

In the forbidden light of atomic hydrogen gas, their secret dance is revealed: we see both the Magellanic stream, a long filament of gas trailing behind the clouds by as much as 100 kpc; and the Magellanic bridge, a tenuous connection between the two galaxies (see figure 1). Such bridge/stream structures are the tell-tale signs of past gravitational encounters: we see them often in both numerical simulations of colliding galaxies, and in many examples of close galaxy pairs throughout the Universe. The Magellanic system is by far the nearest such example, and so studying the residue of their encounter gives us a unique opportunity to study such collisions in great detail.

However, there is something quite mysterious about the tidal debris of the Magellanic system: while the contours of the Magellanic stream and Magellanic bridge are well-traced by atomic hydrogen gas, they seem to be completely devoid of tidally-stripped stars. Indeed, there are no known stars associated with the Magellanic stream, and while there are stars in the Magellanic bridge, as of yet the stars detected in the bridge have been exclusively young. This means they cannot have been tidally stripped as stars during the encounter that formed the

bridge, because in that case, we would see the same admixture of stellar ages that we see in the Clouds themselves. Observationally, if the stars in the bridge had been tidally stripped, we should see a prominent red giant branch associated with the Magellanic bridge, because both clouds possess an abundant population of old red giant stars.

The search for tidally-stripped stars in the Magellanic system is not a trivial exercise in intergalactic bean-counting. The lack of tidally-stripped stars in the bridge and stream calls into question our basic understanding of their gravitational dance. If the structures we see in atomic hydrogen are indeed due to tidal interactions, then the tidal forces which produced them really should have stripped both stars and gas from the clouds into these structures.

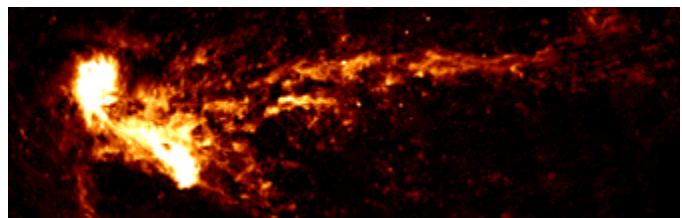


Figure 1: The distribution of HI gas in the Magellanic system. The LMC and SMC are the bright white blobs on the left of the image. They are connected by a bridge of HI gas, and trailed by the Magellanic stream, which extends more than 100 degrees behind the clouds. Image credit: Mary Putman

*continued*

*The Magellanic Bridge continued*

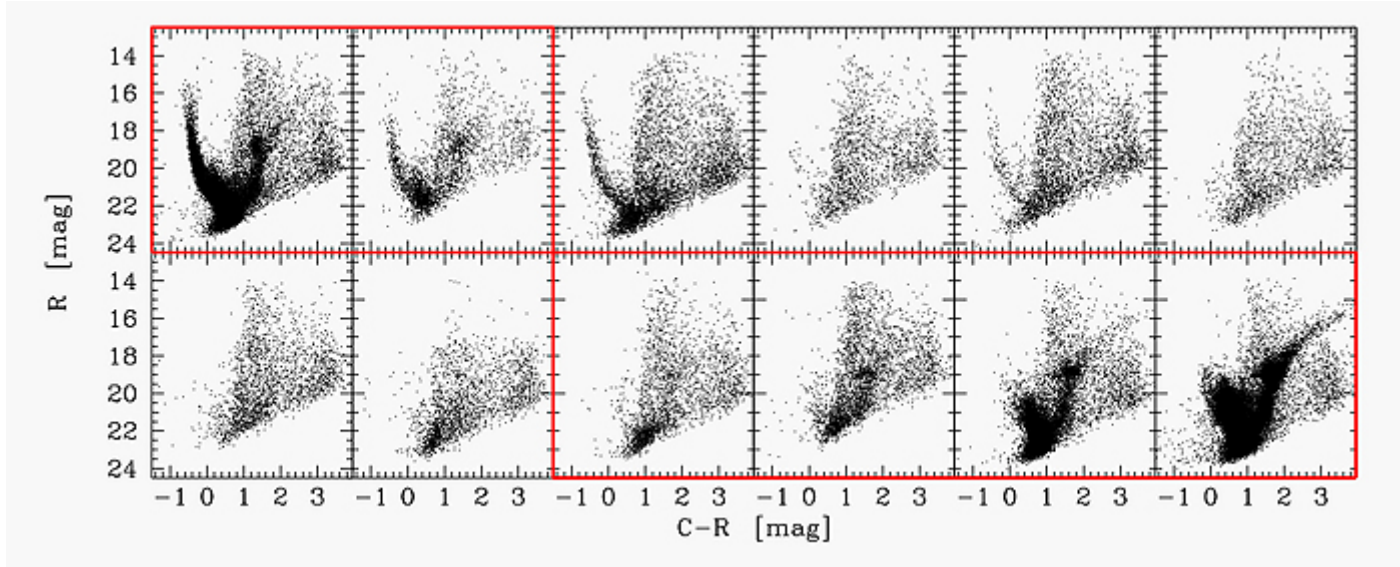


Figure 2: Color-magnitude diagrams for the 12 fields observed in the Magellanic bridge. The fields cover the inter-cloud region, from very near the SMC (upper left panel) to very near the LMC (lower right panel). I found a significant population of red giant stars only in the six fields nearest the SMC or LMC; these fields are outlined in red in the figure online.

**Searching for Red Giants**

In 2006, I used the Mosaic II camera at the CTIO Blanco 4-meter telescope to look for a tidally-stripped population of old red giant stars in the Magellanic Bridge. I obtained deep images of 12 fields spanning the inter-Cloud region, and constructed color-magnitude diagrams (CMDs) of the stellar populations therein (see figure 2).

These CMDs show that some of the fields do indeed possess a red giant population. However, only those fields that are close to either the LMC or SMC show red giant stars. The fields in the central regions of the Bridge do not show red giant branch stars. I conclude from this that the red giants in the “bookend” fields are components of the LMC or SMC, and are not associated with the Bridge. In fact, the surface density profile of red giants in the four fields nearest the LMC is perfectly consistent with previous measurements of the LMC’s exponential disk.

From my 4-meter observations, it certainly looks as if there are no tidally-stripped stars in the Magellanic Bridge. However, there’s one more potential plot-twist: the 12 fields I observed were strung along the HI filament of the Bridge like beads on a string. By restricting my search for red giants to these fields, I am inherently assuming that the tidally-stripped stars will be embedded in the tidally-stripped gas. This is a reasonable assumption, but it is conceivable that the stars and gas could have been separated after having been stripped, because the stripped gas will feel hydrodynamic drag forces from its motion through the Milky Way halo that the stripped stars would not feel.

To address this possibility, I mined the archive of the 2-micron All-Sky Survey (2MASS), constructing near-infrared CMDs for two sections of the inter-Cloud region. One section is coincident with the four of my 4-meter fields that are nearest the LMC. This is my control

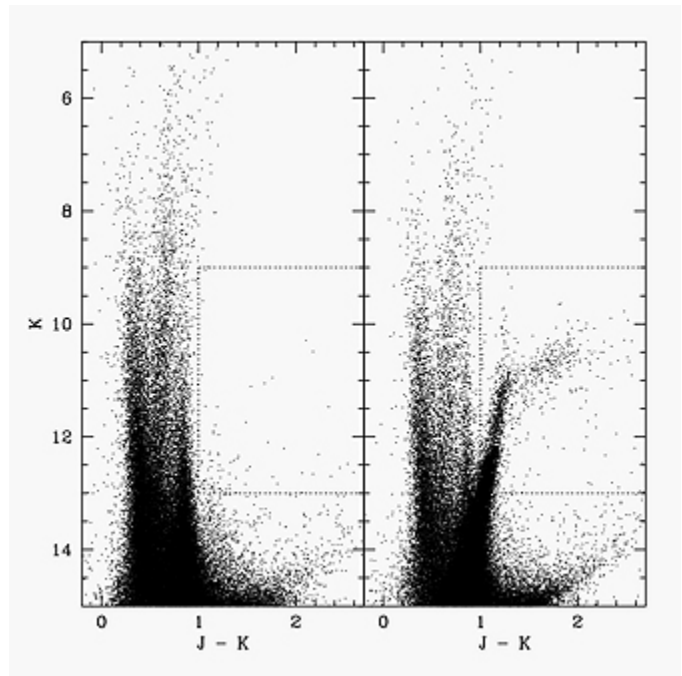


Figure 3: Near-infrared CMDs from 2MASS of two sections of the inter-cloud region: a large central area where bridge giants would be expected (left), and a smaller control area known to contain red giants belonging to the LMC (right). The dotted box in each panel highlights the region occupied by red giants and other evolved stellar populations.

*continued*

## The Magellanic Bridge continued


field, because I know these fields are “polluted” by red giant stars that belong to the LMC. The other section is larger than the control section by a factor of 10, and subtends the entire central portion of the inter-Cloud region, where I found no red giants in my 4-meter fields. By comparing these two CMDs from 2MASS (figure 3), it is immediately obvious that the red giant population seen in the control field is completely absent in the much larger central field. This result confirms that there is no tidally-stripped stellar population associated with the Magellanic Bridge.

### The Young Bridge Population

It is somewhat confounding that there are no tidally-stripped stars in the Bridge; however, the upshot of this realization is that we now know that the young stars present in the Bridge must have formed in situ, from gas which had already been stripped out of the Clouds. That makes the Bridge stars by far the nearest example of stars formed in the wake of a tidal encounter, so they represent a golden opportunity to study tidally-triggered star formation in great detail. In addition, if we can measure the ages of the Bridge stars, we will have determined the timing of the tidal encounter itself, which has important implications for understanding the orbits of the Clouds, and their relationship to each other and to the Milky Way.

I have developed a star formation history analysis code (StarFISH) that can robustly determine the mixture of stellar ages present in a color-magnitude diagram, through statistical comparison with theoretical models. I applied StarFISH to the young stellar populations in the Bridge, and found that star formation was ignited between 200 and 300 Myr ago. Thus the tidal encounter that produced the Bridge must have occurred about 300 Myr ago.

How are we to understand a gravitational encounter between the Magellanic Clouds that selectively stripped only gas from the Clouds, leaving their stars intact? Since gravitational forces do not discriminate between stars and gas, there must have been a bias in the initial configuration of gas and stars in the pre-collision Clouds.

One plausible scenario is that the SMC possessed an envelope of HI gas that extended to much larger radii than its stellar population. Such HI envelopes are not unheard of among dwarf galaxies, so this is a plausible idea. Still, it may be difficult to understand how such a gas envelope could come to be if the LMC and SMC are long-term dance partners. In that case, we might expect that such an extended gas envelope would have been truncated by encounters long before 300 Myr ago. 

# The NEWFIRM Medium-Band Survey

Pieter van Dokkum (Yale), Danilo Marchesini (Yale), Ivo Labbé (OCIW), Gabriel Brammer (Yale), Ryan Quadri (Leiden), Mariska Kriek (Princeton), Marijn Franx (Leiden), Garth Illingworth (UCSC), Kyoung-Soo Lee (Yale), Adam Muzzin (Yale), Gregory Rudnick & Kate Whitaker (Yale)

There is good evidence that galaxy evolution was much more rapid in the 2.5 Gyr interval  $1.5 < z < 3.5$  than in the 10 Gyr since  $z=1.5$ . This epoch was characterized by strong starbursts, spectacular merging activity, and rapid black hole growth (e.g., Rudnick et al., 2006; Daddi et al., 2007). At the same time, some galaxies were not forming new stars at all (e.g., Kriek et al., 2006), even though gas and triggers for star formation were plentiful at this epoch. There was a much greater diversity of galaxies than in today’s Universe, which looks somewhat humdrum in comparison.

Unfortunately, it is difficult to study representative galaxy samples at these early times, as familiar rest-frame optical spectral features are shifted into the near-infrared. Most studies of high-redshift galaxies have focused on blue star-forming galaxies, as they are relatively bright at optical (rest-frame ultraviolet) wavelengths (e.g., Steidel et al., 1996). However, the majority of massive galaxies are relatively red, and much too faint in the observer’s optical for spectroscopy (e.g., van Dokkum et al., 2006). As a result, we either have to work with small, bright samples for which we can obtain near-IR spectra (see Kriek et al., 2008 for our Gemini survey of massive galaxies at  $z \sim 2.5$ ), or rely on photometric redshifts derived from broadband photometry (e.g., Dickinson et al., 2003; Fontana et al., 2006, and many other studies). Although these photometric redshifts are sufficiently accurate for determining broad characteristics of galaxies (such as their luminosity function), they cannot be used to measure accurate rest-frame colors, stellar population parameters, or the local galaxy density.

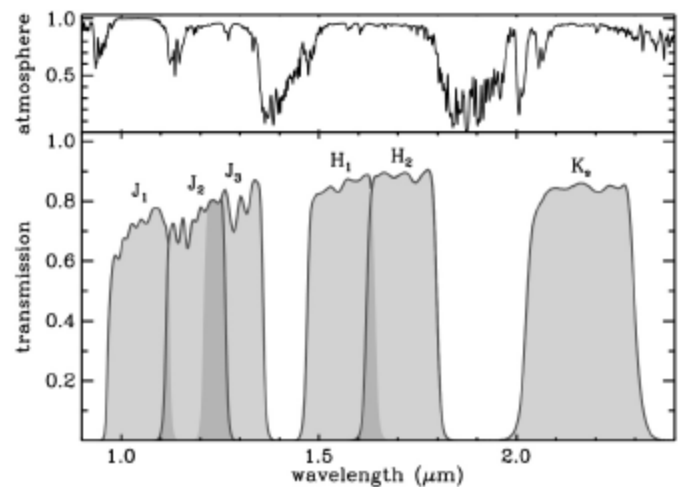


Figure 1: The transmission curves of the medium-band filter system that we designed and manufactured for NEWFIRM. The  $J_1$ ,  $J_2$ ,  $J_3$ ,  $H_1$ , and  $H_2$  filters together provide crude “spectra” with resolution  $R \sim 10$  over the wavelength range 1-1.8 microns, offering a compromise between spectroscopy and broadband imaging.

*continued*

## The NEWFIRM Medium-Band Survey continued

Inspired by the successful Classifying Objects by Medium-Band Observations 17-filter survey (COMBO-17), an optical medium-band imaging survey at redshifts  $0 < z < 1$  (Wolf et al., 2003), we are undertaking a project which will provide a sample of K-selected galaxies with accurate redshifts in the range  $1.5 < z < 3.5$  that is several orders of magnitude larger than what is available today.

We designed and manufactured a set of five custom medium-band near-IR filters for the NEWFIRM wide-field infrared imager on the Kitt Peak Mayall 4-meter telescope, which provide “spectra” with a resolution of  $R \sim 10$  from 1-1.8 microns. The filters, shown in figure 1, pinpoint the location of the redshifted Balmer or 4000 Å break for galaxies at  $1.5 < z < 3.5$ . Combined with broad-band optical- and  $K_s$ -band photometry, these filters should provide redshifts accurate to  $\Delta(1+z) = 0.02-0.03$  at  $z > 1.5$ , a factor of 3–4 better than is possible with broadband photometry alone.

This redshift accuracy is sufficient to isolate the sequence of “red and dead” galaxies in color-magnitude diagrams of high- $z$  galaxies. Furthermore, by combining the redshifts with 2D spatial information, the local galaxy density can be determined, and the improved sampling of the Balmer-break region provides good constraints on the ages of the galaxies.

We proposed to do a deep NEWFIRM survey with these filters in fields that have excellent available data at other wavelengths. The NOAO Survey Time Allocation Committee generously awarded 34 nights. This allocation has been augmented by 30 nights through a WYNN/NOAO time trade. The primary fields are 28 arcmin x 28 arcmin areas in COSMOS and AEGIS. When the survey is completed, we will provide the reduced data to the community, as well as photometric catalogs, redshifts, stellar population parameters, and other ancillary products.

Our first run comprised 24 nights in a single block in March and April. Organizing the run was a fun challenge, with eight observers coming in at various times, a dedicated laptop and 6 terabytes of disk space for on-site reductions, and a wiki page where we kept our night logs, cookbooks, and a host of other information. We were very impressed with NEWFIRM: its wide field and excellent sensitivity are a delight, particularly to those of us who have many nights of experience with older, smaller field-of-view imagers on other telescopes! Despite somewhat mediocre seeing, the run was a success, in large part due to the stability of NEWFIRM and the excellent support of NOAO staff.

Figure 2 shows an example of the type of data we are collecting for thousands of galaxies. The left panel shows broad-band photometry from the NOAO Mosaic imager (optical) and the Infrared Side Port Imager (ISPI) (J, H, and  $K_s$ ) of a galaxy in the Multiwavelength Survey by Yale-Chile (MUSYC) Sloan Digital Sky Survey (SDSS) 1030 field (Quadri et al., 2007). The galaxy is bright in the near-IR ( $K_s = 19.0$ ), but very faint in the optical ( $R = 25.0$ ). Using the photometric redshift code EAZY (Brammer et al., 2008), we derived a broad-band photometric redshift of  $z_{\text{broad}} = 2.27^{+0.19}_{-0.46}$ . This redshift places the object

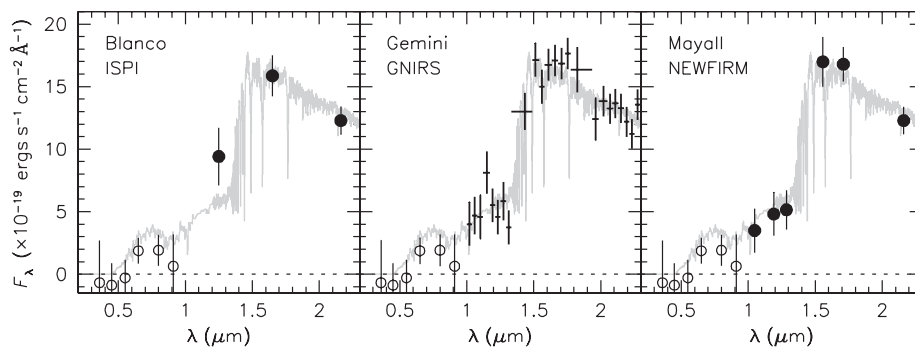


Figure 2: Comparison of “standard” broadband photometry from ISPI on the CTIO Blanco 4-meter telescope (left panel), near-infrared spectroscopy with the cross-dispersed GNIRS spectrograph on Gemini (middle panel), and medium-band imaging with NEWFIRM on the Kitt Peak Mayall 4-meter telescope (right panel). The grey model spectrum (repeated in each panel) is the best fit to the GNIRS data. The resolution offered by the medium-band filters is sufficient to locate the strong Balmer break in this galaxy.

in the range  $1.81 < z < 2.46$  with 68 percent confidence, corresponding to an uncertainty of 0.8 mag in luminosity distance and of 1 Gyr in look-back time.

We had selected this object for follow-up spectroscopy with the cross-dispersed Gemini Near-Infrared Spectrograph (GNIRS). The binned Gemini spectrum is shown in the middle panel (from Kriek et al., 2006, 2008). The spectrum shows no emission lines but a prominent Balmer break, providing the first direct evidence of “red and dead” massive galaxies in the early universe. The location of the break places the galaxy at  $z_{\text{gnirs}} = 2.56^{+0.14}_{-0.02}$ , just outside the confidence interval of the broadband data. The (very preliminary!) NEWFIRM medium-band data for this object are shown in the right panel. The filters unambiguously identify the strong Balmer break between the  $J_3$  and  $H_1$  filters, and the EAZY photometric redshift is  $z_{\text{nmbs}} = 2.64^{+0.08}_{-0.13}$ , a factor of three improvement in accuracy compared to the broadband redshift.

The NEWFIRM data in figure 2 represent only ~40 minutes of exposure time with each of the filters. In our primary fields, we already exceed this by factors of 10–20, and we expect to have photometry of comparable quality for all  $K_s < 21.5$  objects in the NEWFIRM fields when the survey is completed. As no similar studies are currently planned with other telescopes, the final archive of well-sampled spectral energy distributions and accurate redshifts for thousands of faint objects will be a unique resource for studies of the high-redshift universe.  $\blacksquare$

### References

- Brammer, G., van Dokkum, P., & Coppi, P. 2008, ApJ, submitted
- Daddi, E., et al. 2007, ApJ, 670, 173
- Dickinson, M., Papovich, C., Ferguson, H., & Budavári, T. 2003, ApJ, 587, 25
- Fontana, A., et al. 2006, A&A, 459, 745
- Kriek, M., et al. 2006, ApJ, 649, L71
- Kriek, M., et al. 2008, ApJ, 677, 219
- Quadri, R., et al. 2007, AJ, 134, 1103
- Rudnick, G., et al. 2006, ApJ, 650, 624
- Steidel, C., Giavalisco, M., Pettini, M., Dickinson, M., & Adelberger, K. 1996, ApJ, 462, L17
- van Dokkum, P., et al. 2006, ApJ, 638, L59
- Wolf, C., Meisenheimer, K., Rix, H.-W., Borch, A., Dye, S., & Kleinheinrich, M. 2003, A&A, 401, 73